

The effects of normobaric and hyperbaric oxygenation on MRI signal intensities in T_1 -weighted, T_2 -weighted and FLAIR images in human brain

Vida Velej^{1,2}, Ksenija Cankar¹, Jernej Vidmar^{1,3}

¹ Institute of Physiology, Faculty of Medicine, University of Ljubljana, Ljubljana, Slovenia

² Kranj Community Health Center, Gorenjska Basic Healthcare, Kranj, Slovenia

³ Institute of Radiology, University Medical Center Ljubljana, Ljubljana, Slovenia

Radiol Oncol 2023; 57(3): 317-324.

Received 29 May 2023

Accepted 24 July 2023

Correspondence to: Prof. Ksenija Cankar, D.M.D., Ph.D., Institute of Physiology, Faculty of Medicine, University of Ljubljana, Zaloška cesta 4, SI-1000 Ljubljana, Slovenia. E-mail: ksenija.cankar@mf.uni-lj.si

Disclosure: No potential conflicts of interest were disclosed.

This is an open access article distributed under the terms of the CC-BY li-cense (<https://creativecommons.org/licenses/by/4.0/>).

Background. Dissolved oxygen has known paramagnetic effects in magnetic resonance imaging (MRI). The aim of this study was to compare the effects of normobaric oxygenation (NBO) and hyperbaric oxygenation (HBO) on human brain MRI signal intensities.

Patients and methods. Baseline brain MRI was performed in 17 healthy subjects (mean age 27.8 ± 3.2). MRI was repeated after exposure to the NBO and HBO at different time points (0 min, 25 min, 50 min). Signal intensities in T_1 -weighted, T_2 -weighted images and fluid attenuated inversion recovery (FLAIR) signal intensities of several intracranial structures were compared between NBO and HBO.

Results. Increased T_1 -weighted signal intensities were observed in white and deep grey brain matter, cerebrospinal fluid (CSF), venous blood and vitreous body after exposure to NBO as well as to HBO compared to baseline (Dunnett's test, $p < 0.05$) without significant differences between both protocols. There was also no significant difference in T_2 -weighted signal intensities between NBO and HBO. FLAIR signal intensities were increased only in the vitreous body after NBO and HBO and FLAIR signal of caudate nucleus was decreased after NBO (Dunnett's test, $p < 0.05$). The statistically significant differences in FLAIR signal intensities were found between NBO and HBO (paired t-test, $p < 0.05$) in most observed brain structures (paired t-test, $p < 0.05$).

Conclusions. Our results show that NBO and HBO alters signal intensities T_1 -weighted and FLAIR images of human brain. The differences between NBO and HBO are most pronounced in FLAIR imaging.

Key words: hyperbaric oxygen; normobaric oxygen; magnetic resonance; human brain

Introduction

Magnetic resonance imaging (MRI) of brain is a superior soft-tissue contrast method that is used for the assessment of a numerous neurological conditions such as multiple sclerosis and headaches, and used to characterize strokes and space-occupying lesions. Basic MRI brain screen protocol is a sim-

ple non-contrast MRI comprising a group of basic MRI sequences when imaging the brain in cases of no particular condition is being sought (e.g. headache). The protocol is designed to obtain a good general overview of the brain. A standard screening protocol might include T_1 weighted imaging for anatomical overview, T_2 weighted imaging to evaluate basal cisterns, ventricular system and

subdural spaces, and good visualization of flow voids in vessels, fluid attenuated inversion recovery imaging (FLAIR) to assess white-matter, diffusion weighted imaging (DWI) for multiple possible purposes (from the identification of ischemic stroke to the assessment of active demyelination).

Dissolved oxygen can be used as a contrast agent in MRI due to the paramagnetic properties of the dioxygen molecule O_2 .¹ Since O_2 as well as hydroxyl and superoxide radicals contain unpaired electrons, they exhibit paramagnetic effect and may shorten the spin-lattice relaxation time (T_1) in magnetic resonance imaging (MRI).²⁻⁶ T_1 relaxation times shortening under the influence of increased partial pressure of oxygen (pO_2) in the inspired gas mixture is called tissue-oxygen-level-dependent effect (TOLD). It was observed in many tissues: arterial blood, myocardium, spleen, skeletal muscles, renal cortex, liver and fat.^{4,7-9} TOLD effect was also detected in brain parenchyma (grey and white matter) and cerebrospinal fluid (CSF).¹⁰⁻¹⁶ In addition, pO_2 increase also affects spin-spin relaxation time (T_2)^{13,17}; however, results of available studies on the effect of pO_2 on T_2 relaxation times are controversial.^{7,12} FLAIR images of healthy volunteers also showed increased CSF signal intensity during 100% oxygen breathing.¹⁸

Concentration of dissolved oxygen is directly proportional to its partial pressure, pO_2 .¹⁹ High pO_2 values in arterial blood as well as in brain parenchyma can be achieved with normobaric 100% oxygenation (NBO) compared to breathing normobaric air (NBA). Hyperbaric 100% oxygenation (HBO) causes a more pronounced increase of arterial and brain pO_2 compared to NBO as well as augments production of reactive oxygen species (ROS).²⁰⁻²² In few animal studies, it has been already observed that HBO had a more pronounced effect on T_1 and T_2 relaxation times compared to breathing NBO or NBA.^{11,23}

To our knowledge, no human studies were performed studying the effect of HBO on MRI signal intensities. The aim of this study was to compare the effects of HBO and NBO on MRI signal intensities (e.g. T_1 , T_2 and FLAIR).

Patients and methods

The study was approved by The National Ethics Committee (No. 0120-203/2019/4). Research was conducted at the Institute of Physiology (University of Ljubljana, Faculty of Medicine). Informed consent was obtained from each subject.

17 healthy volunteers (12 males and 5 females), age 20–40 years (mean age 27.8 ± 3.2), were enrolled in the study. Exclusion criteria were: history of a neurological disorder, non-MRI-compatible devices, a lung disease with FEV1/FVC < 60% and/or emphysema and/or pneumothorax, history of middle ear trauma or disease, therapy with platinum complexes, doxorubicin, bleomycin, disulfiram or mafenide acetate, pregnancy or claustrophobia.

Study protocol

MRI examination was performed before oxygen breathing protocol (baseline state), after HBO and after NBO with subsequent MRI on separate visits. NBO protocol was performed using a non-rebreather oxygen mask connected to a large reservoir supplied by 100% oxygen for 70 minutes. HBO protocol was performed in multiplace hyperbaric chamber (Kovinarska P&P, Slovenia) at 2.4 ATA with breathing of 100% oxygen for 70 minutes as shown in Figure 1. After each oxygen breathing protocol (NBO or HBO), MRI examination was repeated three times, i.e. immediately after the end of HBO or NBO, after 25 min and after 50 min.

MR image acquisition

The MRI imaging was performed on a 3T MRI system (TX Achieva Philips Netherlands) with the use of a 32-channel head coil. The MR examination consisted of:

- T_1 spin echo (SE) imaging in the transversal plane with imaging parameters: repetition time (TR) 1026 ms, echo time (TE) 10 ms, field of view (FOV) 230×183 mm, matrix 256×163 , voxel 0.9×1.12 mm, slice thickness 4 mm, gap 1 mm, number of slices 29, number of signals averaged (NSA) 2 with approximate duration of 5 min 38 s
- T_2 turbo spin echo (TSE) imaging in the transversal plane with imaging parameters: TR 9179 ms, TE 100 ms, FOV 230×185 mm, matrix 384×229 , voxel 0.6×0.75 mm, slice thickness 3 mm, gap 0 mm, number of slices 50, NSA 3, sensitivity (SENS) 1.7 with approximate duration of 4 min 55 s.
- FLAIR in transversal plane: TR 11000 ms, TE 125 ms, TI 2800 ms, FOV 230×183 mm, matrix 328×185 , voxel 0.7×0.93 mm, slice thickness 3 mm, gap 1 mm, number of slices 36, NSA 2, SPIR technique, SENS 2 with approximate duration: 3 min 51 s.

The total MRI scanning time during one MR examination was 25 min.

MR data and statistical analysis

The MRI images were analysed using ImageJ free image analysis software (National Institutes of Health, USA). Mean signal values in distinct regions of interest (ROI) on T_1 -weighted, T_2 -weighted and FLAIR images were obtained: frontal white matter, thalamus, caudate nucleus, putamen, hippocampus, superior sagittal sinus, vitreous body and cerebrospinal fluid (CSF).

Statistical analysis was performed using SigmaPlot 14.0 (Systat Software, Inc., USA). The signal intensities after NBO or HBO were compared to the baseline values. Shapiro-Wilk test and Brown-Forsythe were used to check for normality and equal variance. One-way repeated measurements analysis of variance (RM ANOVA) was used to test for differences between signal intensities before, immediately, 25 min and 50 min after NBO or HBO. In cases when Shapiro-Wilk or Brown-Forsythe test failed, Friedman RM ANOVA on Ranks was performed. If RM ANOVA showed statistically significant differences between groups of data,

Breathing protocol in hyperbaric chamber

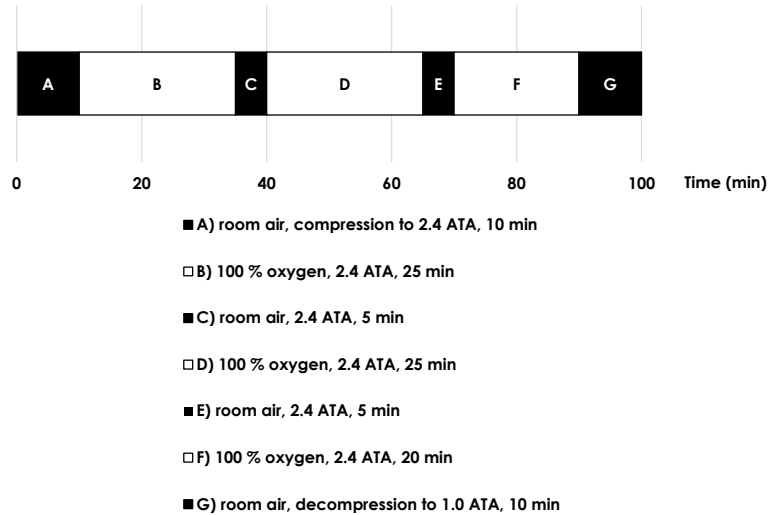


FIGURE 1. Hyperbaric oxygenation (HBO) protocol.

Dunnett’s method for multiple comparisons was used to compare signal intensities at three time

TABLE 1. Comparison of T_1 -weighted signal intensities before, immediately, 25 min and 50 min after normobaric oxygenation (NBO) (A) and hyperbaric oxygenation (HBO) (B) (mean ± standard deviation)

A) NBO					
Structure	Baseline	0 min	25 min	50 min	p
Frontal white matter	770.1 ± 251.2	791.0 ± 238.4	837.3 ± 328.4	851.3 ± 337.7*	0.044
Thalamus	827.9 ± 275.6	846.7 ± 244.7	894.6 ± 338.4	914.7 ± 356.5*	0.038
Head of caudate nucleus	731.9 ± 238.3	753.8 ± 227.0	798.7 ± 318.8	820.9 ± 331.3*	0.023
Putamen	800.2 ± 257.0	814.2 ± 239.2	860.7 ± 333.8	878.1 ± 350.2	0.059
Hippocampus	701.6 ± 232.0	712.1 ± 211.3	751.8 ± 285.5	771.6 ± 303.8*	0.038
Superior sagittal sinus	818.0 ± 375.6	748.2 ± 252.1	778.3 ± 288.6	860.9 ± 304.8	0.019
Cerebrospinal fluid	356.6 ± 126.8	362.7 ± 108.5	396.6 ± 152.9*	397.7 ± 163.0*	0.010
Vitreous body	281.3 ± 89.6	288.0 ± 92.1	296.8 ± 115.0	302.5 ± 116.3	0.264
B) HBO					
Structure	Baseline	0 min	25 min	50 min	p
Frontal white matter	770.1 ± 251.2	834.7 ± 133.0	860.9 ± 158.9	886.6 ± 184.7*	0.026
Thalamus	827.9 ± 275.6	900.8 ± 147.1	933.3 ± 169.1	957.1 ± 193.9*	0.004
Head of caudate nucleus	731.9 ± 238.3	794.9 ± 124.4	819.9 ± 142.4	846.2 ± 173.7	0.013
Putamen	800.2 ± 257.0	867.1 ± 134.9	893.9 ± 154.6	922.5 ± 185.1*	0.007
Hippocampus	701.6 ± 232.0	764.8 ± 124.1	787.2 ± 142.1	807.5 ± 163.2	0.044
Superior sagittal sinus	818.0 ± 375.6	848.0 ± 227.8	911.9 ± 310.7	907.6 ± 335.0	0.127
Cerebrospinal fluid	356.6 ± 126.8	396.4 ± 60.2	400.7 ± 73.7	413.0 ± 98.9	0.256
Vitreous body	281.3 ± 89.6	361.2 ± 63.0*	335.9 ± 69.6	349.4 ± 82.8	0.040

*statistically significant difference compared to baseline value at p < 0.05; NBO = 100 % normobaric oxygen, HBO = 100 % hyperbaric oxygen

points after oxygen breathing protocol with baseline values. Additionally, RM ANOVA or Friedman RM ANOVA on Ranks was used to check for differences in signal values of each ROI in T_1 -weighted, T_2 -weighted and FLAIR images between baseline signal values and values after HBO/NBO at each time point (0 min, 25 min, 50 min). The signal intensity changes in T_1 -weighted, T_2 -weighted and FLAIR images compared to baseline in each ROI at each time point (0 min, 25 min, 50 min) after NBO and HBO were calculated. Paired t-test was used to compare the signal intensity changes at each time point between NBO and HBO. In cases when Shapiro-Wilk normality test failed, Wilcoxon signed rank test was performed. The α level was set at $p < 0.05$ for all statistical significances.

Results

The results of T_1 -weighted signal intensities before, immediately, 25 min and 50 min after NBO or HBO are presented in Table 1. After NBO there was a

statistically significant increase in T_1 -weighted signal intensity in all studied structures except for vitreous body and putamen (RM ANOVA, Dunnett's test, $p < 0.05$). In contrast, after HBO we observed a significant increase in T_1 -weighted signal intensities except for the superior sagittal sinus and CSF (Dunnett's test, $p < 0.05$). T_1 -weighted signal intensity was significantly higher immediately (0 min) as well as 25 min after the end of the HBO compared to T_1 -weighted signal intensity immediately and 25 min after NBO in vitreous body (paired t-test, $p < 0.05$). In contrast, there was no difference in signal intensities in T_1 -weighted images between HBO and NBO after 50 min.

The results of T_2 -weighted signal intensities before, immediately, 25 min and 50 min after NBO or HBO are presented in Table 2. T_2 -weighted signal intensities were increased only in frontal white matter and thalamus after NBO and in the superior sagittal sinus and vitreous body after HBO (Dunnett's test, $p < 0.05$). There was also no significant difference in T_2 -weighted signal intensities between HBO and NBO.

TABLE 2. Comparison of T_2 -weighted signal intensities before, immediately, 25 min and 50 min after normobaric oxygenation (NBO) (A) and hyperbaric oxygenation (HBO) (B) (mean \pm standard deviation)

A) NBO					
Structure	Baseline	0 min	25 min	50 min	p
Frontal white matter	362.5 \pm 33.1	367.8 \pm 32.8	397.1 \pm 80.4*	389.0 \pm 51.3*	0.007
Thalamus	480.6 \pm 49.6	485.1 \pm 63.5	521.0 \pm 114.8	508.0 \pm 61.7	0.022
Head of caudate nucleus	621.8 \pm 64.8	637.9 \pm 54.0	673.6 \pm 139.8	656.7 \pm 91.4	0.631
Putamen	514.0 \pm 57.0	527.7 \pm 50.7	552.3 \pm 103.4	542.2 \pm 64.1	0.073
Hippocampus	694.9 \pm 71.9	712.6 \pm 83.5	756.9 \pm 190.3	734.0 \pm 98.2	0.281
Superior sagittal sinus	41.3 \pm 6.8	42.7 \pm 8.6	45.7 \pm 12.5	45.0 \pm 11.3	0.317
Cerebrospinal fluid	1996.8 \pm 143.6	2059.7 \pm 203.3	2171.2 \pm 522.0	2107.9 \pm 274.3	0.318
Vitreous body	1404.8 \pm 114.8	1499.4 \pm 159.1	1585.5 \pm 396.5	1520.9 \pm 224.1	0.080
B) HBO					
Structure	Baseline	0 min	25 min	50 min	p
Frontal white matter	362.5 \pm 33.1	359.4 \pm 26.7	367.0 \pm 35.5	375.1 \pm 44.7	0.223
Thalamus	480.6 \pm 49.6	473.6 \pm 34.4	479.3 \pm 33.3	489.1 \pm 59.1	0.365
Head of caudate nucleus	621.8 \pm 64.8	617.8 \pm 47.3	620.9 \pm 50.0	639.5 \pm 77.1	0.390
Putamen	514.0 \pm 57.0	510.9 \pm 37.1	514.6 \pm 39.8	532.9 \pm 65.4	0.256
Hippocampus	694.9 \pm 71.9	695.9 \pm 57.2	688.1 \pm 38.4	713.4 \pm 81.4	0.378
Superior sagittal sinus	41.3 \pm 6.8	48.3 \pm 14.0*	47.4 \pm 11.8	48.0 \pm 15.0	0.047
Cerebrospinal fluid	1996.8 \pm 143.6	1972.3 \pm 79.2	1984.8 \pm 102.3	2027.9 \pm 195.4	0.482
Vitreous body	1404.8 \pm 114.8	1524.0 \pm 114.7*	1529.5 \pm 143.2*	1530.9 \pm 189.8*	0.001

* statistically significant difference compared to baseline value at $p < 0.05$; NBO = 100 % normobaric oxygen; HBO = 100 % hyperbaric oxygen

The results of FLAIR signal intensities before, immediately, 25 min and 50 min after NBO or HBO are presented in Table 3. FLAIR signal intensities were increased only in the vitreous body after NBO and HBO, signal of caudate nucleus was decreased after NBO (Dunnett's test, $p < 0.05$).

The statistically significant differences in FLAIR signal intensities were found between NBO and HBO (paired t-test, $p < 0.05$) in caudate nucleus, thalamus, hippocampus and vitreous body at each time point (0 min, 25 min, 50 min). In addition, the differences were also observed between NBO in HBO in putamen and frontal white matter at 0 min and 25 min and in superior sagittal sinus at 25 min (paired t-test, $p < 0.05$).

Discussion

In the present study we observed increased signal intensity in T_1 -weighted imaging in frontal white matter, thalamus, caudate nucleus and hippocampus after NBO as well as HBO, in superior sagittal sinus and CSF after NBO and in vitreous body and putamen after HBO. Additionally, signal intensity was increased in T_2 -weighted imaging in frontal white matter and thalamus after NBO as well as in superior sagittal sinus and vitreous body after HBO. FLAIR signal intensities were increased only in the vitreous body after NBO and HBO. In contrast, FLAIR signal of caudate nucleus was decreased after NBO. Statistically significant differences between HBO and NBO were observed in FLAIR signal intensities of caudate nucleus, vitreous body, putamen, frontal white matter, hippocampus and thalamus and also in T_1 -weighted signal intensity of vitreous body.

In our study, T_1 -weighted signal intensity of brain structures increased progressively with time after NBO/HBO and was the highest 50 min after the end of both, HBO and NBO. This finding is in agreement with the paramagnetic effect of O_2 . Increased level of dissolved paramagnetic molecular O_2 shortens T_1 -relaxation times due to dipole-dipole interactions and increases signal intensity on T_1 -weighted images.^{4,7-16 23 24} Relaxation rate ($R_1 = 1/T_1$) increases proportionally with increasing pO_2 in inspired gas mixture, the increase being linear or logarithmic when in normobaric or hyperbaric conditions, respectively.^{23,24} The various increase of T_1 -weighted signal intensities in the observed tissues might be explained by increased microvascular pO_2 as well as by differences in tissue oxygenation.⁷ The sustained increase in T_1 -weighted

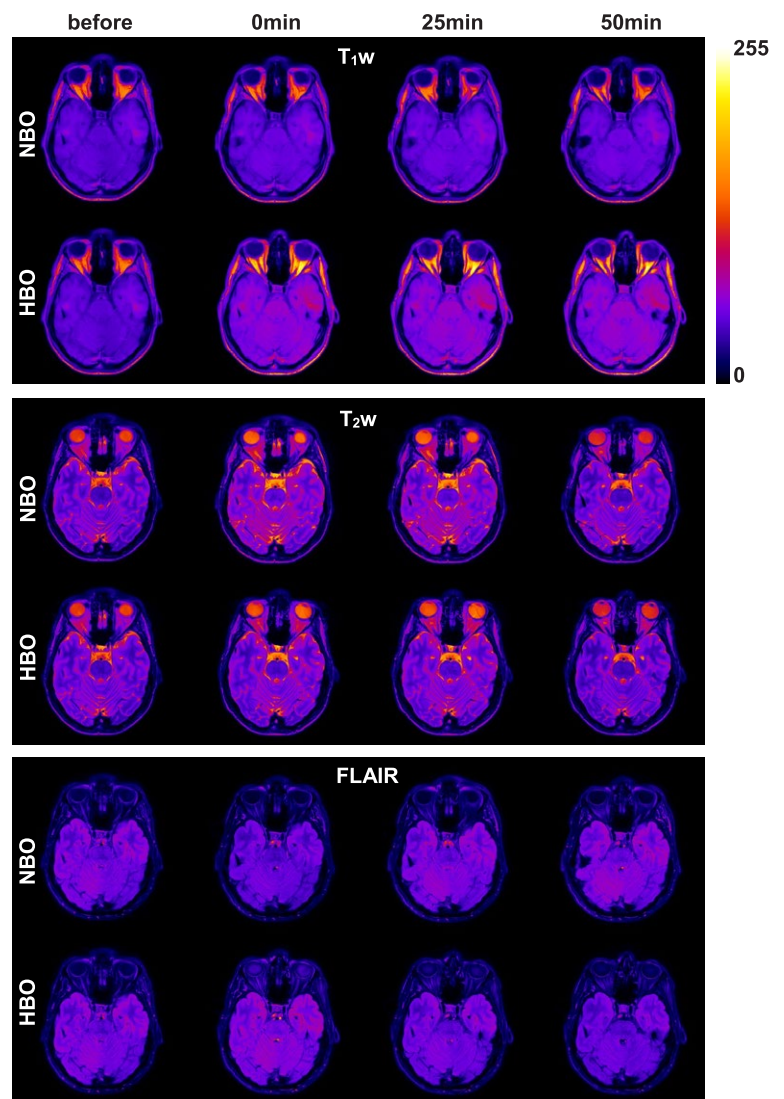


FIGURE 2. Representative MRI images in healthy subject at baseline, immediately after the end, after 25 min and after 50 min of NBO or HBO.

signal intensity is further supported by a study of Rockswold *et al.* which showed significantly elevated brain tissue pO_2 30 min after the end of HBO and NBO.²⁵ In contrast to Rockswold *et al.*, we failed to observe a peak in T_1 -weighted signal intensity immediately after the end of oxygen therapy. A possible explanation is that the time delay between HBO/NBO and MRI was too long to detect the peak.

We observed progressive increase in T_1 -weighted signal intensities after both NBO and HBO along with MRI imaging time, with the highest signal increase at the end of imaging protocol. This phenomenon could not be attributed solely to changes in pO_2 , but also to the effect of ROS on

TABLE 3. Comparison of FLAIR signal intensities before, immediately, 25 min and 50 min after normobaric oxygenation (NBO) (A) and hyperbaric oxygenation (HBO) (B) (mean \pm standard deviation)

A) NBO					
Structure	Baseline	0 min	25 min	50 min	p
Frontal white matter	731.7 \pm 77.0	700.8 \pm 89.8	713.7 \pm 125.1	717.4 \pm 128.7	0.615
Thalamus	897.1 \pm 101.7	851.5 \pm 96.7	868.6 \pm 164.3	861.5 \pm 153.6	0.399
Head of caudate nucleus	1119.2 \pm 131.9	1083.0 \pm 129.4	1070.0 \pm 213.0	1030.0 \pm 172.5*	0.039
Putamen	928.1 \pm 116.5	875.8 \pm 129.0	893.2 \pm 184.3	893.0 \pm 171.4	0.354
Hippocampus	1216.2 \pm 135.7	1162.1 \pm 144.8	1173.5 \pm 223.0	1174.1 \pm 239.1	0.490
Superior sagittal sinus	91.2 \pm 23.6	84.6 \pm 23.5	78.2 \pm 27.2	86.0 \pm 33.2	0.299
Cerebrospinal fluid	139.6 \pm 33.3	140.5 \pm 39.8	147.0 \pm 51.8	157.8 \pm 53.2	0.228
Vitreous body	127.2 \pm 29.4	170.4 \pm 49.1*	157.3 \pm 45.0*	147.3 \pm 45.9	0.002
B) HBO					
Structure	Baseline	0 min	25 min	50 min	p
Frontal white matter	731.7 \pm 77.0	755.8 \pm 113.1	794.7 \pm 135.2	782.2 \pm 115.3	0.508
Thalamus	897.1 \pm 101.7	927.1 \pm 104.6	691.3 \pm 127.3	949.7 \pm 110.5	0.973
Head of caudate nucleus	1119.2 \pm 131.9	1180.6 \pm 183.3	1208.0 \pm 175.8	1190.8 \pm 152.3	0.508
Putamen	928.1 \pm 116.5	958.3 \pm 143.4	993.0 \pm 148.2	978.9 \pm 133.4	0.567
Hippocampus	1216.2 \pm 135.7	1269.4 \pm 171.3	1294.4 \pm 184.7	1286.7 \pm 160.4	0.771
Superior sagittal sinus	91.2 \pm 23.6	93.4 \pm 25.8	105.1 \pm 30.5	106.4 \pm 37.0	0.193
Cerebrospinal fluid	139.6 \pm 33.3	134.5 \pm 27.0	139.4 \pm 20.2	138.3 \pm 21.8	0.909
Vitreous body	127.2 \pm 29.4	691.4 \pm 142.9*	523.6 \pm 122.9*	378.1 \pm 88.8	< 0.001

* statistically significant difference compared to baseline value at $p < 0.05$; NBO = 100 % normobaric oxygen; HBO = 100 % hyperbaric oxygen

T_1 and T_2 -weighted images. Since ROS such as hydroxyl and superoxide radicals contain unpaired electrons, they also exhibit strong paramagnetic effect (a strong T_1 relaxation times shortening) and only a small, statistically insignificant reduction of T_2 relaxation times.^{5,6} Additional point to consider is that distinct neurons respond to oxidative stress differently^{26,27}, which leads us to presumption that the effect of HBO-induced oxidative stress would lead to different levels of ROS and thus different effect on T_1 and T_2 weighted signal intensities in various brain regions.

The increase of T_1 -weighted signal intensities was more pronounced in frontal white matter and thalamus after HBO compared to NBO. This could be explained by altered O_2 diffusion after HBO. We observed increased signal intensity in superior sagittal sinus and CSF only after NBO, but not after HBO. Longer time delay between HBO and MRI most likely lowered pO_2 in the aforementioned fluids before the beginning of MRI. We showed that T_1 -weighted signal intensity of vitreous body was significantly increased immediately after

the end of HBO exposure and then decreased in subsequent imaging blocks. This is in accordance with expected pO_2 dynamics in vitreous body, described by Shui *et al.*²⁸ Surprisingly, after the exposure to NBO, no increase in vitreous T_1 -weighted signal intensity was observed. A possible explanation is that lower vitreous pO_2 (as achieved during NBO compared to HBO) dropped to baseline level before the beginning of the MRI.

In our study, there were statistical differences in T_2 -weighted signal intensities between baseline and after NBO in frontal white matter and thalamus. This is in accordance with Wu *et al.* who observed significant differences in T_1 and T_2 between grey and white matter after inhalation of NBO.¹² According to Wu *et al.*, T_2 relaxation time increases in rat brain with hyperoxia. In contrast, Tadamura *et al.* did not observe this effect in human "non-brain" tissues (myocardium, spleen, liver, subcutaneous fat, skeletal muscle and bone marrow).⁷ Therefore, it is possible that the effect of hyperoxia on T_2 -weighted signal intensities appears to vary in different tissues. In the present study, a signifi-

cant increase in T_2 -weighted signal intensities was also observed after HBO in superior sagittal sinus and vitreous body. Oxygen affects spin-spin relaxation time (T_2) by two competing mechanisms, i.e. T_2 shortening analogous to effect on T_1 (although the effect on T_2 is much smaller) and T_2 lengthening due to diffusion of water protons through field inhomogeneities induced by deoxyhemoglobin generated field gradients (blood-oxygen-level-dependent (BOLD) effect).^{13,17} An increased T_2 -weighted signal intensity after NBO and HBO in our study suggests that in human brain structures and vitreous body the paramagnetic effect of oxygen on T_2 relaxation times shortening prevails over BOLD effect.

Our results show statistically significant differences between HBO and NBO were observed in FLAIR signal intensities in different brain structures particularly those that are close to CSF spaces. These results are in accordance with previous studies which showed that in patients receiving 100% NBO elevated pO_2 leads to incomplete signal suppression of CSF in FLAIR imaging.^{29,30} The elevated pO_2 most likely favors O_2 entry into the CSF not through the choroid plexus but directly through the walls of arteries and arterioles on the brain surface.³⁰ Since in HBO there is up to 2.5 times higher pO_2 , this effect in FLAIR imaging is more pronounced. We observed increase in FLAIR signal of vitreous body immediately after HBO/NBO exposure and then a subsequent decrease in time – again, this is in accordance with expected pO_2 dynamics in vitreous body, as described by Shui *et al.*²⁸

The results of the present study could have also some clinical implications. Namely, the prolonged intubation induces changes of signal intensities in T_1 -weighted and FLAIR images of brain MRI³¹ similar as those observed in our study after NBO. Knowing that prolonged oxygenation induces paramagnetic effects in brain tissues as observed in our study, it is important to take this into account when interpreting brain MRI in intubated patients or in patients after HBO therapy.

The present study has several limitations. First, we failed to show significant differences in MRI signal intensities in brain structures after HBO compared to NBO. It would be expected that brain tissue pO_2 is significantly higher after HBO compared to NBO²¹ due to higher concentration of dissolved O_2 during HBO.¹⁹ The only exception was T_1 -weighted signal intensity of vitreous body immediately and 25 min after HBO compared to NBO. One possible explanation is that MRI was

performed with time delay of 15 minutes after the end of HBO due to logistics. Perhaps with shorter time delay the peak in T_1 -weighted signal intensities could be observed similarly as in the study of Rockswold *et al.*²⁵ Additionally, the present study was semiquantitative using clinical head MRI protocol and the next step would be more quantitative approach using T_1 mapping and T_2 mapping. Furthermore, we did not measure brain tissue pO_2 nor levels of ROS, which would help to explain the observed changes in signal intensities in T_1 -weighted and T_2 -weighted images. Since our study was performed *in vivo* in a group of volunteers measuring of brain tissue pO_2 seems rather controversial. We could only measure pO_2 in arterial blood, however these results do not reflect brain tissue pO_2 directly. However, according to the reference, at 3 ATA pO_2 in arterial blood increases to nearly 270 kPa and in tissue to above 53 kPa.³² In contrast, in NBO conditions, partial pressure of pO_2 in the brain is expected to be only between 4 - 6.4 kPa according to study of Meixensberger *et al.*³³ These values are much lower than during HBO. Therefore, we expected similar tissue pO_2 differences between HBO and NBO in the present study protocol.

In conclusion, the increased T_1 -weighted signal intensities were observed in white and grey brain tissues, brain fluids and vitreous body after NBO as well as HBO, without significant differences between both protocols. In addition, the structure limited and diverse signal intensity increase was observed in T_2 -weighted imaging and FLAIR after NBO and HBO. However, the prospective quantitative studies are needed to further clarify the effects of NBO and HBO breathing on MRI in human brain.

References

1. McGrath DM, Naish JH, O'Connor JP, Hutchinson CE, Waterton JC, Taylor CJ, et al. Oxygen-induced changes in longitudinal relaxation times in skeletal muscle. *Magn Reson Imaging* 2008; **26**: 221-7. doi: 10.1016/j.mri.2007.06.011
2. Bloch F, Hansen WW, Packard M. The nuclear induction experiment. *Phys Rev* 1946; **70**: 474-85. doi: DOI 10.1103/PhysRev.70.474
3. Chiarotti G, Cristiani G, Giulotto L. Proton relaxation in pure liquids and in liquids containing paramagnetic gases in solution. *Nuovo Cimento* 1955; **1**: 863-73. doi: Doi 10.1007/BF02731333
4. Young IR, Clarke GJ, Bailes DR, Pennock JM, Doyle FH, Bydder GM. Enhancement of relaxation rate with paramagnetic contrast agents in NMR imaging. *J Comput Tomogr* 1981; **5**: 543-7. doi: 10.1016/0149-936x(81)90089-8
5. Tain RW, Scotti AM, Li W, Zhou XJ, Cai K. Influence of free radicals on the intrinsic MRI relaxation properties. *Adv Exp Med Biol* 2017; **977**: 73-9. doi: 10.1007/978-3-319-55231-6_11

6. Tain RW, Scotti AM, Li W, Zhou XJ, Cai K. Imaging short-lived reactive oxygen species (ROS) with endogenous contrast MRI. *J Magn Reson Imaging* 2018; **47**: 222-9. doi: 10.1002/jmri.25763
7. Tadamura E, Hatabu H, Li W, Prasad PV, Edelman RR. Effect of oxygen inhalation on relaxation times in various tissues. *J Magn Reson Imaging* 1997; **7**: 220-5. doi: 10.1002/jmri.1880070134
8. Ding Y, Mason RP, McColl RW, Yuan Q, Hallac RR, Sims RD, et al. Simultaneous measurement of tissue oxygen level-dependent (TOLD) and blood oxygenation level-dependent (BOLD) effects in abdominal tissue oxygenation level studies. *J Magn Reson Imaging* 2013; **38**: 1230-6. doi: 10.1002/jmri.24006
9. O'Connor JP, Naish JH, Jackson A, Waterton JC, Watson Y, Cheung S, et al. Comparison of normal tissue R1 and R2* modulation by oxygen and carbon. *Magn Reson Med* 2009; **61**: 75-83. doi: 10.1002/mrm.21815
10. Haddock B, Larsson HB, Hansen AE, Rostrup E. Measurement of brain oxygenation changes using dynamic T(1)-weighted imaging. *Neuroimage* 2013; **78**: 7-15. doi: 10.1016/j.neuroimage.2013.03.068
11. Muir ER, Cardenas D, Huang S, Roby J, Li G, Duong TQ. MRI under hyperbaric air and oxygen: effects on local magnetic field and relaxation times. *Magn Reson Med* 2014; **72**: 1176-81. doi: 10.1002/mrm.25027
12. Wu Y, Gao X, Feng X, Tao X, Tang CY. Oxygen-enhanced magnetic resonance imaging of the brain: a rodent model. *Neuroreport* 2012; **23**: 581-4. doi: 10.1097/WNR.0b013e328353a4bb
13. Uematsu H, Takahashi M, Hatabu H, Chin CL, Wehrli SL, Wehrli FW, et al. Changes in T1 and T2 observed in brain magnetic resonance imaging with delivery of high concentrations of oxygen. *J Comput Assist Tomogr* 2007; **31**: 662-5. doi: 10.1097/rct.0b013e3180319114
14. Kettunen MI, Grohn OH, Silvennoinen MJ, Penttonen M, Kauppinen RA. Effects of intracellular pH, blood, and tissue oxygen tension on T1rho relaxation in rat brain. *Magn Reson Med* 2002; **48**: 470-7. doi: 10.1002/mrm.10233
15. Remmele S, Sprinkart AM, Muller A, Traber F, von Lehe M, Gieseke J, et al. Dynamic and simultaneous MR measurement of R1 and R2* changes during respiratory challenges for the assessment of blood and tissue oxygenation. *Magn Reson Med* 2013; **70**: 136-46. doi: 10.1002/mrm.24458
16. Zaharchuk G, Martin AJ, Rosenthal G, Manley GT, Dillon WP. Measurement of cerebrospinal fluid oxygen partial pressure in humans using MRI. *Magn Reson Med* 2005; **54**: 113-21. doi: 10.1002/mrm.20546
17. Thulborn KR, Waterton JC, Matthews PM, Radda GK. Oxygenation dependence of the transverse relaxation-time of water protons in whole-blood at high-field. *Biochim Biophys Acta* 1982; **714**: 265-70. doi: 10.1016/0304-4165(82)90333-6
18. Anzai Y, Ishikawa M, Shaw DW, Artru A, Yarnykh V, Maravilla KR. Paramagnetic effect of supplemental oxygen on CSF hyperintensity on fluid-attenuated inversion recovery MR images. *AJNR Am J Neuroradiol* 2004; **25**: 274-9. PMID: 14970030
19. Taylor CD. Solubility of oxygen in a seawater medium in equilibrium with a high-pressure oxy-helium atmosphere. *Undersea Biomed Res* 1979; **6**: 147-54. PMID: 531994
20. Whalen RE, Saltzman HA, Holloway DH, Jr., McIntosh HD, Sieker HO, Brown IW Jr. Cardiovascular and blood gas responses to hyperbaric oxygenation. *Am J Cardiol* 1965; **15**: 638-46. doi: 10.1016/0002-9149(65)90350-4
21. Daugherty WP, Levasseur JE, Sun D, Rockswold GL, Bullock MR. Effects of hyperbaric oxygen therapy on cerebral oxygenation and mitochondrial function following moderate lateral fluid-percussion injury in rats. *J Neurosurg* 2004; **101**: 499-504. doi: 10.3171/jns.2004.101.3.0499
22. Poff AM, Kernagis D, D'Agostino DP. Hyperbaric environment: Oxygen and cellular damage versus protection. *Compr Physiol* 2016; **7**: 213-34. doi: 10.1002/cphy.c150032
23. Matsumoto K, Bernardo M, Subramanian S, Choyke P, Mitchell JB, Krishna MC, et al. MR assessment of changes of tumor in response to hyperbaric oxygen treatment. *Magn Reson Med* 2006; **56**: 240-6. doi: 10.1002/mrm.20961
24. Kinoshita Y, Kohshi K, Kunugita N, Tosaki T, Yokota A. Preservation of tumour oxygen after hyperbaric oxygenation monitored by magnetic resonance imaging. *Br J Cancer* 2000; **82**: 88-92. doi: 10.1054/bjoc.1999.0882
25. Rockswold SB, Rockswold GL, Zaun DA, Zhang X, Cerra CE, Bergman TA, et al. A prospective, randomized clinical trial to compare the effect of hyperbaric to normobaric hyperoxia on cerebral metabolism, intracranial pressure, and oxygen toxicity in severe traumatic brain injury. *J Neurosurg* 2010; **112**: 1080-94. doi: 10.3171/2009.7.JNS09363
26. Baek BS, Kwon HJ, Lee KH, Yoo MA, Kim KW, Ikono Y, et al. Regional difference of ROS generation, lipid peroxidation, and antioxidant enzyme activity in rat brain and their dietary modulation. *Arch Pharm Res* 1999; **22**: 361-6. doi: 10.1007/Bf02979058
27. Wang X, Michaelis EK. Selective neuronal vulnerability to oxidative stress in the brain. *Front Aging Neurosci* 2010; **2**: 12. doi: 10.3389/fnagi.2010.00012
28. Shui YB, Fu JJ, Garcia C, Dattilo LK, Rajagopal R, McMillan S, et al. Oxygen distribution in the rabbit eye and oxygen consumption by the lens. *Invest Ophthalmol Vis Sci* 2006; **47**: 1571-80. doi: 10.1167/iov.05-1475
29. Braga FT, da Rocha AJ, Hernandez G, Arikawa RK, Ribeiro IM, Fonseca RB. Relationship between the concentration of supplemental oxygen and signal intensity of CSF depicted by fluid-attenuated inversion recovery imaging. *Am J Neuroradiol* 2003; **24**: 1863-8. PMID: 14561617
30. Deliganis AV, Fisher DJ, Lam AM, Maravilla KR. Cerebrospinal fluid signal intensity increase on FLAIR MR images in patients under general anesthesia: the role of supplemental O2. *Radiology* 2001; **218**: 152-6. doi: 10.1148/radiology.218.1.r01ja43152
31. Frigon C, Jardine DS, Weinberger E, Heckbert SR, Shaw DW. Fraction of inspired oxygen in relation to cerebrospinal fluid hyperintensity on FLAIR MR imaging of the brain in children and young adults undergoing anesthesia. *AJR Am J Roentgenol* 2002; **179**: 791-6. doi: 10.2214/ajr.179.3.1790791
32. Leach RM, Rees PJ, Wilmshurst P. Hyperbaric oxygen therapy. *BMJ* 1998; **317**: 1140-3. doi: 10.1136/bmj.317.7166.1140
33. Meixensberger J, Dings J, Kuhnigk H, Roosen K. Studies of tissue PO2 in normal and pathological human brain cortex. *Acta Neurochir Suppl* 1993; **59**: 58-63. doi: 10.1007/978-3-7091-9302-0_10